

## N O T I C E

THIS DOCUMENT HAS BEEN REPRODUCED FROM  
MICROFICHE. ALTHOUGH IT IS RECOGNIZED THAT  
CERTAIN PORTIONS ARE ILLEGIBLE, IT IS BEING RELEASED  
IN THE INTEREST OF MAKING AVAILABLE AS MUCH  
INFORMATION AS POSSIBLE

(NASA-TN-79276) TENSILE AND FLEXURAL  
STRENGTH OF NON-GRAPHITIC SUPERHYBRID  
COMPOSITES: PREDICTIONS AND COMPARISONS  
(NASA) 27 p HC A03/NP A01

CSCL 11D

63/24

NSO-11100

Unclass  
46049

# TENSILE AND FLEXURAL STRENGTH OF NON- GRAPHITIC SUPERHYBRID COMPOSITES: PREDICTIONS AND COMPARISONS

C. C. Chamis, J. H. Sinclair, and R. F. Lark  
Lewis Research Center  
Cleveland, Ohio



Prepared for the  
Eleventh National Technical Conference  
sponsored by the Society for the Advancement of Material and  
Process Engineering  
Boston, Massachusetts, November 13-15, 1979

# TENSILE AND FLEXURAL STRENGTH OF NONGRAPHITIC SUPERHYBRID COMPOSITES: PREDICTIONS AND COMPARISONS

by C. C. Chamis, J. H. Sinclair, and R. F. Lark  
National Aeronautics and Space Administration  
Lewis Research Center  
Cleveland, Ohio

## Abstract

Equations are presented and described which can be used to predict bounds on the tensile and flexural strengths of nongraphitic superhybrid (NGSH) composites. These equations are derived by taking into account the measured stress-strain behavior, the lamination residual stresses and the sequence of events leading to fracture. The required input for using these equations includes constituents, properties (elastic and strength), NGSH elastic properties, cure temperature, and ply stress influence coefficients. Results predicted by these equations are in reasonably good agreement with measured data for strength and for the apparent "knees" in the nonlinear stress-strain curve. The lower bound values are conservative compared to measured data. These equations are relatively simple and are suitable for use in the preliminary design and initial sizing of structural components made from NGSH composites.

## 1. INTRODUCTION

The superhybrid (SH) composite concept<sup>(1,2)</sup> provides a means for efficiently utilizing advanced materials by using the best characteristics of fiber/resin matrix composites, fiber/metal matrix composites, and high strength metallic foils combined in a single adhesively bonded laminate. Typically, SH composites are made by using titanium foil outer plies over boron/aluminum (B/Al) plies with graphite fiber/epoxy (Gr/E) plies in an inner core which has a titanium ply in the center. Both B/Al and Gr/E plies have the fibers in the same direction which is referred to, herein, as the longitudinal direction (1-axis) of

the laminate. The transverse direction (2-axis) is 90° to the fiber direction, and the thickness direction is normal to the 1-2 plane. Another approach is to make the inner core plies from nongraphitic composites such as S-glass/epoxy (S-G/E) or Kevlar/49/epoxy (KEV-E). These types of superhybrids are referred to as nongraphitic superhybrids (NGSHs). The NGSHs considered in this investigation are listed in table 1. The feasibility for making NGSHs and assessing their mechanical properties as well as their advantages, disadvantages, and possible areas of SAMPE paper.<sup>(3)</sup> Photomicrographs of the cross-sections of the various NGSHs investigated, and schematics of speci-

men geometry with instrumentation arrangement are shown in reference 3.

Comparisons of results between predicted and measured elastic properties (moduli and Poisson's ratios) were also included in that paper. In order to consider NGSs for structural applications and assess their effectiveness through the preliminary design phase, methods for predicting their strength properties are needed. The objective of this paper is to develop and describe methods which can be used to predict the tensile and flexural strengths of NGSs.

These methods embody simple equations which predict (estimate) upper and lower bounds on longitudinal and transverse tensile strengths, and on longitudinal and transverse flexural strengths. They also embody simple equations which can be used to predict (estimate) the "knees" in the transverse tension nonlinear stress-strain curves. These equations are derived by taking into account the measured stress-strain behavior, the calculated lamination residual stresses, and the probable sequence of events leading to fracture as determined by calculated ply stresses. The required input for using these equations consists of constituent composite elastic and strength properties, NGS elastic properties, and ply stress influence coefficients (PSICs). The results predicted by these equations, for the NGSs listed in table 1, are compared with measured data to assess the accuracy of the predictions.

Preliminary design and initial sizing of structural components from NGSs requires knowledge of other strengths such as compression, shear, and impact resistance as well as fatigue, and environmental effects. Description of comparable methods for predicting compression strengths, shear strengths and impact resistance is lengthy and will be dealt with in a sequel paper.

## 2. LAMINATION RESIDUAL STRESSES

The lamination residual stresses in the NGSs considered were determined using the linear laminate theory and combined-stress failure criteria available in an existing computer code.<sup>(4)</sup> Briefly, this laminate theory predicts elastic and thermal properties of the laminate based on the properties of the plies. Alternatively, the theory predicts stresses (strains) in the plies when the laminate stress (strain) is known. The combined-stress strength criterion is derivable from a modified distortion energy principle for a three dimensional solid and accounts for different strengths in the different directions and also for different strengths in tension and compression. The temperature difference used for these calculations was 300° F which is the difference between a cure temperature of 370° F and the test temperature of 70° F. The constituent materials properties used in the computer code to calculate the lamination residual stresses in the plies are summarized in table 2. The results obtained are summarized in table 3.

The MOS (Margin of Safety) columns in this table represent the margin between the combined residual stress and the combined available strength in a particular ply as predicted by the failure criteria.<sup>(4)</sup> "Zero" or negative MOS values indicate ply failure. Negative MOS values are obtained for the S-G/E and the KEV/E plies in all the NGS laminates. Comparing ply residual stresses from table 3 with corresponding ply strengths in table 2, it is seen that: (1) the residual transverse ply stress in the KEV/E plies is about 5 ksi and is about 5 times the corresponding ply strength (about 1 ksi), and (2) is about the same in the S-G/E plies.

The point to be noted is that the lamination residual stresses are sufficiently high to produce transply cracks in the S-G/E and KEV/E plies in all the NGSs. The formation of transply cracks relieves the residual stresses

in these plies and prevents them from supporting transverse stress due to mechanical load. All of these effects are significant and fundamental for predicting the strength of the NGSs.

### 3. TENSILE STRENGTH PREDICTIONS

The information used to predict the tensile strength of the NGSs and the prediction procedure for strengths and for stress-strain behavior are described in this section.

#### 3.1 STRESS-STRAIN AND POISSON'S STRAIN CURVES

Stress-strain curves and Poisson's strain curves were determined for all the NGSs tested. Typical computer-plotted curves<sup>(5)</sup> obtained by averaging data from back-to-back 0°-90° strain gage rosettes (located at mid length center of the specimen) are shown in figures 1 to 7 for both longitudinal and transverse loadings. The information from these figures pertinent to strength predictions is that the longitudinal curves are linear to fracture (or nearly so) for all the NGSs while the transverse curves are nonlinear. The transverse curves (fig. 1) show an initial linear portion up to the first knee. This is relatively small (about 0.1 percent strain). It is followed by a long nonlinear region from the first to the second knee, and a short more pronounced nonlinear region from the second knee to fracture.

#### 3.2 PLY STRESSES

The ply stresses calculated at laminate measured fracture load using the computer code<sup>(4)</sup> are summarized in table 4.

Examining first the ply stresses due to longitudinal load, it is seen that the MOS is negative for both the titanium and B/Al plies and is relatively large in positive value (greater than 0.5 compared to "0" for imminent fracture) for the adhesive, S-G/E, or KEV/E. The negative MOS values for the titanium

plies resulted from using the yield stress (120 ksi, table 2) as allowable in the combined-stress calculations. Using the ultimate tensile (160 ksi) the MOS is slightly negative for the S-G(DT) and S-G(DCT) NGSs and positive for the other five. The longitudinal stresses in the titanium plies range from 136 to 170 ksi and average to about 150 ksi which is 6 percent less than the ultimate tensile strength of the titanium (160 ksi). These results indicate that the ultimate tensile strength of the titanium should be used in the combined stress strength criterion. The longitudinal stresses in the B/Al plies range from 247 to 334 ksi and average about 290 ksi which is about 32 percent higher than the uniaxial tensile strength of 220 ksi in table 2. The longitudinal stresses in the adhesive, S-G/E or KEV/E plies are less than 50 percent of their corresponding strengths in table 2. The increase in strength in the B/Al plies compared to the uniaxial strength is probably due to in situ enhancement or "synergistic effect."

The above observations suggest that the B/Al plies fail first. The titanium plies probably fail shortly thereafter. The S-G/E or KEV/E plies most likely fail very rapidly (dynamically) from the large stresses in these plies induced by the redistribution of the load. This information then provides a basis for formulating lower and upper bounds on longitudinal strength for NGSs as will be described later.

It is seen in table 4 that the B/Al, the S-G/E, and the KEV/E plies have large negative MOS values. On the other hand, the titanium plies and the adhesive plies have MOS values near unity. The transverse ply stresses in the B/Al plies are from 2 to 5 times greater than the corresponding ply strengths shown in table 2. The transverse ply stresses in either the S-G/E or KEV/E plies are also greater than their corresponding ply strengths. In contrast, the transverse ply stress in either the titanium or adhesive plies is relatively small

compared to the corresponding ply strength.

The above observations suggest that the B/Al plies fail first (first knee of stress-strain curve, fig. 1). Next, the titanium plies yield (second knee) and finally fail by ultimate tension. Neither the S-G/E nor the KEV/E plies contribute significantly to the transverse strength of the NGSH. These plies have probably already failed by the lamination residual stress as was mentioned previously. As a result of this failure sequence the laminate stress-strain curve should exhibit two knees. The first of these occurs at relatively small strains, when the B/Al plies fail, and the second near fracture when the titanium plies yield. This is consistent with the transverse stress-strain curves described previously. The procedure for predicting the stresses associated with the two knees will be described later.

### 3.3 PLY STRESS INFLUENCE COEFFICIENTS FOR IN-PLANE STRESSES

The ply stress influence coefficients (PSIC) provide a convenient means for predicting laminate longitudinal and transverse strengths of superhybrids. These coefficients were used successfully to predict the fracture stresses (strength) of Titanium/Beryllium (Tiber) hybrids.<sup>(6)</sup> The PSICs for the NGSH of interest are summarized in table 5. These coefficients show that the B/Al plies carry the major portion of the longitudinal stresses. Compared to the B/Al the other plies participate in supporting laminate longitudinal stress as follows: titanium plies, about 50 percent; S-G/E or KEV/E plies, about 25 percent; and the adhesive only about 8 percent.

The PSICs show that the B/Al and titanium plies carry about the same and practically all of the laminate transverse tensile stress. Compared to the stresses carried by these plies the S-G/E plies carry about 20 percent,

the KEV/E plies about 3 percent and the adhesive plies about 1 percent.

The points to be noted from the above observations are: (1) the major portion of the NGSH laminate transverse stress is carried by the titanium and B/Al plies, and (2) the adhesive plies carry very little stress in both the longitudinal and transverse directions. Both of these conditions are fundamental characteristics of the superhybrid concept.

### 3.4 PREDICTION OF BOUNDS FOR IN-PLANE LONGITUDINAL AND TRANSVERSE STRENGTHS

The method used to predict the laminate in-plane longitudinal and transverse tensile strengths of similar to that used successfully in reference 6. This method is relatively simple and yields only upper and lower bounds of the strengths. In order to use this method, the PSICs (table 5) and the properties of the constituents and the NGSHs summarized in table 6 are needed as described below.

Longitudinal. The equations for predicting the bounds of the longitudinal tensile strength ( $S_{GH}$ ) are based on the following assumptions:

- (1) The longitudinal tensile stress-strain curve is linear to fracture. This is consistent with the measured stress-strain curves (figs. 1 to 7).
- (2) The NGSH modulus ( $E_{GH}$ ) is predictable from the constituents properties using linear laminate theory. The predicted longitudinal moduli, using linear laminate theory, are in reasonably good agreement with measured data as is discussed in reference 3.
- (3) The effects of lamination residual stress on NGSH strength is negligible. Recall from section 2 that the lamination residual stresses were of sufficiently high magnitude to produce transply cracks in either

the S-G/E or KEV/E (resin-composite) plies and thereby reduce the effects of the lamination residual stresses.

- (4) The adhesive has sufficient strength to preserve composite action of all the constituents in the NGSHs up to, or immediately prior to, fracture. This assumption is supported by the collective results in tables 3, 4, and 5 as was previously discussed.
- (5) The probable sequence of events producing longitudinal tensile fracture is as follows: the B/Al plies fracture first followed by the titanium plies and finally the resin-composite plies fail, most likely dynamically. The calculated ply stresses at fracture in table 4 and the PSICs provide the basis for this assumption as was already mentioned.

The equations derived based on the above assumptions are given by:

Upper bound

$$S_{SH} = \frac{S_{TU}}{I_T} \quad (1)$$

Lower bound

$$S_{SH} = \left( 1 - \frac{t_T}{t_{SH}} \frac{E_T}{E_{SH}} \right) \left( \frac{E_{SH}}{E_{B/Al}} \right) S_{B/Al} + \frac{t_T}{t_{SH}} S_{TU} \quad (2)$$

The notation in equations (1) and (2) is as follows: S denotes strength; E denotes modulus; I denotes PSIC; and t denotes thickness of the subscripts, SH denotes superhybrid, T denotes titanium, U denotes ultimate and B/Al denotes boron/aluminum. Equation (1) indicates that the maximum stress to fracture of the NGSHs is controlled by the ultimate tensile strength of the titanium

plies. Equation (2) indicates that the minimum stress to fracture of the NGSHs is controlled by the tensile strength of the B/Al plies plus the additional stress increment required to fracture the titanium plies in ultimate tension. Note that in both cases the titanium plies are used to the maximum capacity of the material strength since their fracture is controlled by ultimate strength instead of yield as would be the case in conventional use of titanium.

Transverse. The assumptions made to derive equations for predicting the in-plane transverse tensile strength bounds of NGSHs are as follows:

- (1) The adhesive has sufficient strength to preserve composite action of all constituents to fracture. The collective results in tables 3, 4, and 5 support this assumption as was the case for assumption 5 for the longitudinal strength.
- (2) The transverse stress-strain curves are nonlinear to fracture (figs. 1 to 7).
- (3) The resin composite plies contribute insignificantly to the laminate transverse tensile strength due to transply cracks induced by the lamination residual stresses (results tables 3, 4, and 5).
- (4) The probable sequence of events producing transverse tensile fracture is as follows: The B/Al plies fail relatively early (at about 0.1 percent strain) followed by yield in the titanium plies and tensile fracture of the titanium plies shortly thereafter. The calculated transverse ply stresses, table 4, and the PSICs provide the basis for this assumption as was previously mentioned.

The resulting equations for the strength bounds are given by:

Upper bound

$$S_{SH} = \left(1 - \frac{t_T E_T}{t_{SH} E_{SH}}\right) \left(\frac{E_{SH}}{E_{B/AI}}\right) S_{B/AI} + \frac{t_T}{t_{SH}} S_{TU} \quad (3)$$

Lower bound

$$S_{SH} = S_{TU} \frac{t_T}{t_{SH}} \quad (4)$$

The symbols in equations (3) and (4) have the same meaning as those in equations (1) and (2) except that the transverse properties are used. Equation (3) indicates that the maximum transverse strength of NGSs is controlled by the stress required to fail the B/AI plies plus the additional stress increment required to fail the titanium plies in ultimate tension. Equation (4) indicates that the minimum transverse tensile stress of NGSs is controlled by the stress required to fracture the titanium plies in ultimate tension.

#### Strength predictions and comparisons.

The bounds predicted by equations (1), (2), (3), and (4) are summarized in table 7 where the experimentally obtained strengths are also summarized for ease of comparison. The points to be noted from the results in table 7 are:

- (1) The lower bounds are conservative for both longitudinal and transverse strengths.
- (2) The predicted upper bounds are less than the experimental values in 4 of the 14 cases.
- (3) The experimental strength is closer to the upper bound in about half the cases. The difference between the predicted lower bound and the experimental value is attributed, in part, to the contribution of the fiber/resin composite plies. Another part is probably due to the representation of the sequence of

events during fracture in the equations. For example, the B/AI plies may fail in one location but continue to carry load in another. The important observation from the above discussion is that the lower bound predicts longitudinal and transverse strengths of NGSs which are conservative compared to experimental data. These predictions should be suitable for preliminary designs and initial sizing of structural components from NGSs.

### 3.5 TRANSVERSE STRESS-STRAIN BEHAVIOR

The knees in the transverse stress-strain curves (refer to fig. 1) may be estimated using the following equations:

First knee (B/AI plies fail)

$$\sigma_{SH} = \frac{S_{B/AI}}{I_{B/AI}} \quad (5)$$

Second knee (titanium plies yield)

$$\sigma_{SH} = \frac{S_{B/AI}}{I_{B/AI}} \left(1 - I_T \frac{t_T}{t_{SH}}\right) + \frac{t_T}{t_{SH}} S_{TY} \quad (6)$$

where  $\sigma$  denotes stress and the subscript y denotes yield. The remaining notation has already been defined. It is noted that the various knees in the stress-strain curves are significant in design depending on whether the anticipated loads are monotonic or cyclic. The fracture stress is used for the monotonic case, whereas the stress at the first or second knee is used for the cyclic load case.

The stresses estimated using equations (5) and (6), and appropriate values from tables 5 and 6 are summarized in table 8. Those estimated from the corresponding stress-strain curves (figs. 1 to 7) and the transverse strengths from table 7 are also included for comparison purposes. The predicted stresses at the two knees are generally in reasonable agreement with the

experimental data. Some large differences exist. These differences may be caused, in part, by the difficulties in measuring small strains during testing. Note that some of the predicted stresses at the second knee are higher than those predicted for the lower bound strength. This result is significant because it may be used as a criterion for selecting the strength predicted by the upper bound equation. The important point to be noted from the afore-discussion is that the transverse tensile stress-strain behavior of NGSBs can be estimated reasonably well using the equations described herein.

#### 4. FLEXURAL STRENGTH PREDICTIONS

The information used to predict the flexural longitudinal and transverse strengths of NGSBs and the prediction methods (equations and comparisons) are described in this section.

##### 4.1 PLY STRESSES

The calculated ply stresses due to 3-point bending measured fracture load in the outer plies on the tension side of the specimen are summarized in table 9. The MOS of the longitudinal ply stresses indicate failures (negative MOS values) in the titanium and B/Al plies but no failure in the other plies. The MOS of the transverse ply stresses indicate failures in the B/Al and S-G/E or KEV/E plies, imminent failure in the titanium plies or the KEV(TYP) NGSB and no failure in the adhesive plies.

Comparing ply stresses from table 9 with corresponding strengths in table 2 the following can be seen:

- (1) The longitudinal stresses in the titanium plies are approximately equal (on the average) to the ultimate tensile strength (160 ksi) while the transverse stresses are approximately equal to the yield stress (120 ksi).

- (2) The longitudinal stresses in the B/Al plies are about 10 percent greater (on the average) than the tensile strength (220 ksi). The transverse ply stresses, on the other hand, are several times greater (about 3 to 5) than the transverse tensile strength (20 ksi).
- (3) The longitudinal ply stresses in the S-G/T or KEV/E plies are about 25 percent of the corresponding ply strengths, respectively 187 and 200 ksi. In contrast, the transverse ply stresses are about twice the ply strengths.
- (4) The stresses in the adhesive plies are about one-third or less than the tensile strength (6 ksi).

It is also interesting to note that the ply fracture stresses in the titanium and B/Al plies are about the same as those resulting from tensile fracture loads, table 4.

Taken collectively the above observations indicate that the B/Al plies fail first followed by failure of the titanium plies. The other plies fail, probably dynamically, producing specimen fracture. The B/Al plies control longitudinal flexural fracture while the titanium plies control transverse flexural fracture. This provides the basis for deriving the equations to predict upper and lower bounds for longitudinal and transverse flexural strengths.

##### 4.2 FLEXURAL STRENGTHS

The equations for predicting the bounds for longitudinal and transverse flexural strength are based primarily on the same assumptions as those used for predicting longitudinal tensile strength. Some additional assumptions are: (1) the tension and compression elastic properties are equal or almost equal for the constituent plies and the NGSBs, and (2) fracture is initiated on the tensile side of the flexural specimen. The

second assumption is justified since B/Al is stronger in compression than tension.

Longitudinal. The equations for predicting the upper and lower bounds for longitudinal flexural strength are:

Upper bound

$$S_{SH} = \frac{S_{TU}}{I_T} \quad (7)$$

Lower bound

$$S_{SH} = \frac{S_{B/Al}}{I_{B/Al}} \quad (8)$$

where the notation has the same meaning as the previously defined except that the ply stress influence coefficients (PSICs) are those calculated from flexural loading and are summarized in table 10. (Those values in parentheses were used when given.) These influence coefficients show that the B/Al plies load at a faster rate (compared to other plies) in longitudinal tension while the titanium plies load at a faster rate in transverse tension.

Transverse. The equations for predicting the upper and lower bounds for flexural transverse strength are given by:

Upper bound

$$S_{SH} = \frac{S_{TU}}{I_T} \quad (9)$$

Lower bound

$$S_{SH} = \frac{12}{2} (S_{TU} h_T t_T + S_{B/Al} h_{B/Al} t_{B/Al}) \quad (10)$$

where  $h$  is the distance from the neutral plane to the centroid of the outer titanium or B/Al plies on the tension

side of the specimen and  $t$  is the combined thickness of the outer titanium or B/Al plies on the same side;  $h$  is measured to the centroid of a single ply or to the centroid of the combined plies for two or more plies. The other symbols have already been defined.

Equations (7) and (9) show that the maximum flexural strength of NGSBs is achieved where the titanium plies fail in ultimate tension. Equation (8) shows that minimum longitudinal flexural strength is achieved when the B/Al plies fail in longitudinal tension. Equation (10) shows that the minimum transverse flexural strength is reached when the B/Al plies fail in transverse tension and, either simultaneously or an instant later, the titanium plies fail in ultimate tension.

Comparisons. The flexural strengths predicted by equations (7) to (10) are summarized in table 11 together with the experimental data for comparison purposes. The points to be noted in this table are:

- (1) The lower bounds for all the cases except S-G(DCT) longitudinal are conservative compared to experimental data.
- (2) The upper bound is a better estimator of the flexural strength for NGSBs with typical ply configuration.
- (3) The spread between the two bounds for transverse strength is about 37 ksi which is greater than that for the longitudinal (about 17 ksi).

The difference between the lower bound and the experimental value for longitudinal flexural is suspected to be caused by a different fracture mode (interlaminar shear, for example) which was not considered in the present strength predictions.

The important observation from the above discussion is that the equations for lower bound predict conservative but reasonable values for the flexural

strengths of NGSBs provided that fracture is not initiated by interlaminar shear stresses. These equations should be suitable for preliminary designs and initial sizing of structural components made from NGSBs.

## 5. SUMMARY

The major results of an investigation to predict tensile and flexural strength of nongraphitic superhybrids (NGSBs) are as follows:

- (1) The experimental longitudinal stress-strain curves and the Poisson's stress strain curves are linear, or nearly so, to fracture while the transverse ones are nonlinear and exhibit two knees.
- (2) The lamination residual stresses in the adhesive plies and those due to mechanical loads are relatively small compared to the strength of the adhesive. And the adhesive has sufficient remaining strength to maintain the composite action of the constituents.
- (3) The calculated lamination residual stresses are of sufficient magnitude to produce transply cracks in the resin/composite plies. These transply cracks relieve or minimize their effects on the ply stresses due to mechanical loading.
- (4) Calculated ply stresses for both tensile and flexural loadings are sufficiently high to initiate failure in the B/Al plies which is followed by ultimate tensile failure of the titanium plies. Subsequently the resin/composite plies (S-G/E or KEV/E) fail very rapidly (dynamically) due to load redistribution.
- (5) Equations (of relatively simple form) are derived which can be used to predict bounds for the tensile and flexural strengths. The input information to these equations includes: constitu-

ents' properties, NGSB properties and ply stress influence coefficients.

- (6) The predicted stresses at the knees of the transverse stress-strain curves are in reasonable agreement with those estimated from the experimental stress-strain curves.
- (7) The predicted strength bounds are in reasonably good agreement with experimental data. The lower bounds are conservative (provided that interlaminar shear stresses do not initiate fracture) and should be suitable for preliminary design, and/or initial sizing of structural components from NGSBs.

## 6. REFERENCES

1. Chamis, C. C., Lark, R. F., and Sullivan, T. L., "Boron/Aluminum-Graphite/Resin Advanced Fiber Composite Hybrids," NASA TN D-7879 (1975).
2. Chamis, C. C., Lark, R. F., and Sullivan, T. L., "Super-Hybrid Composites - An Emerging Structural Material," NASA TM X-71836 (1975).
3. Lark, R. F., Sinclair, J. H., and Chamis, C. C., "Fabrication and Testing of Nongraphitic Superhybrid Composites," NASA TM 79102 (1979).
4. Chamis, C. C., "Computer Code for the Analysis of Multilayered Fiber Composites-User's Manual," NASA TN D-7013 (1971).
5. Chamis, C. C., Kring, J., and Sullivan, T. L., "Automated Testing Data Reduction Computer Program," NASA TM X-68050 (1972).
6. Chamis, C. C., and Lark, R. F., "Titanium/Beryllium Laminates: Fabrication Mechanical Properties, and Potential Aerospace Applications," NASA TM 73891 (1975).

## 7. BIOGRAPHIES

### C. C. Chamis

Dr. Chamis is a member of the Structures Research Section, Structures Branch, Materials and Structures Division where he has been since 1968. He received his B.S. in Civil Engineering (1960) from Cleveland State, M.S. (1962), and Ph.D (1967) in Engineering Mechanics from Case Western Reserve University where he was a member of the Engineering Design Center. His current research is in the area of analysis, design and optimization of composite structural components. He is also involved in the analysis and design of testing methods for advanced composites. His experience in structural fiber composites dates back to 1962 when he was with the Engineering Analysis group of B. F. Goodrich Research Center. He has authored or co-authored numerous papers in his current areas of research. Dr. Chamis is an Adjunct Professor of Civil Engineering at Cleveland State University. He is a member of the AIAA, ASCE, ASME, ASTM, SAMPE, and Sigma Xi. He is a Registered Professional Engineer in the State of Ohio.

### J. H. Sinclair

Mr. Sinclair is a member of the Structures Research Section, Structures Branch, Materials and Structures Division of the NASA-Lewis Research Center, Cleveland, Ohio. He has been at the NASA-Lewis Research Center since 1956. He received a B.S. degree from Michigan State University. He is currently involved with the testing of composites for the purpose of characterization and the identification of failure modes. He has also performed finite element analysis of complex composite structures including composite laminates, composite blades, and strip hybrids. He is a member of SESA.

### R. F. Lark

Mr. Lark is a member of the Structures Research Section, Structures Branch, Materials and Structures Division of the NASA-Lewis Research Center, Cleveland, Ohio. He has been at the NASA-Lewis Research Center since 1958. He received his B.S. in Chemical Engineering (1948) from Case Institute of Technology. His current work assignment involves the project management of in-house and contractual programs for the development of composite pressure vessels and composite materials for aircraft engine components and wind turbine blades. Other experience includes the development of positive expulsion devices, advanced fibers, resins and adhesives and acoustic emission technology. He has contributed significantly to the advancement in the state-of-the-art of composite pressure vessel and positive expulsion technology and advanced composites in general. He is a member of SAMPE, SPE, and the MIL-HDBK 17 Committee.

TABLE 1. - SUPERHYBRID DESCRIPTION AND DESIGNATION

Super-hybrid designation	Number of plies	Starting sequence
Non-graphitic (NCSH)		
S-G (TYP)	21	TI/ADH/TI/ADH/(B/AI)/ADH/(S-G/E) <sub>2</sub> /ADH/TI (symmetric, see note below)
KEV (TYP)	21	TI/ADH/TI/ADH/(B/AI)/ADH/(KEV/E) <sub>2</sub> /ADH/TI
S-G (MOP)	17	TI/ADH/(B/AI)/ADH/(S-G/E) <sub>2</sub> /AIH/TI
KEV (MOP)	17	TI/ADH/(B/AI)/ADH/(KEV/E) <sub>2</sub> /AIH/TI
S-G (DT)	31	(TI/ADH) <sub>2</sub> /(B/AI)/ADH <sub>2</sub> /(S-G/E) <sub>2</sub> /ADH/TI
KEV (DT)	31	(TI/ADH) <sub>2</sub> /(B/AI)/ADH <sub>2</sub> /(KEV/E) <sub>2</sub> /ADH/TI
S-G (DCT)	29	TI/ADH/TI/ADH/(B/AI)/ADH/(S-G/E) <sub>2</sub> /ADH/TI
Graphitic (GSH)		
AS (TYP)	21	TI/ADH/TI/ADH/(B/AI)/ADH/(AS/E) <sub>2</sub> /ADH/TI

Notes: All super-hybrids are symmetric about the mid-surface of the center titanium ply  
 (TYP) = typical; (MOP) = 3-mill outer ply  
 (DT) = double thickness; (DCT) = double core thickness  
 S-G = glass/epoxy (S-G/E) (0.0053 in. thick)  
 KEV = Kevlar-49/epoxy (KEV/E) (0.0053 in. thick)  
 AS = AS (graphite fiber)/epoxy (AS/E) (0.0050 in. thick)  
 TI = titanium (0.0017 in. thick) (TYP and DCT); 0.0030 in. thick outer plies (MOP and DT)  
 ADH = adhesive (0.0016 in. thick)  
 B/AI = 5.6 mill diameter boron fiber/aluminum (0.0071 in. thick)  
 The thickness of the various plies are shown for configuration comparison.

TABLE 2. - PROPERTIES OF CONSTITUENTS USED IN PREDICTING THE

PROPERTIES OF SUPREHYBRIDS

Property	Units	T1 (6 AL-IV)	Adhesive (FM-1000)	B/AJ (S. G./0001)	S-G/EP	KEV/EP
Density	lb/in <sup>3</sup> (a)	0.16	0.042	0.005	0.077	0.049
Nominal thickness	in(b)	.0017	.0016	.007	.0052	.0061
Fiber volume (approx.)	percent	-----	-----	50	70	53
Modulus	10 <sup>6</sup> psi(c)					
E1		16.0	.20	33.8	8.8	10.0
E2		16.0	.20	21.0	3.6	.65
G12		6.2	.07	7.2	1.7	.36
G13		6.2	.07	7.2	1.7	.36
G23		6.2	.07	6.8	.5	.24
Poisson's ratio						
ν12		.3	.4	.25	.23	.41
ν23		.3	.4	.39	.50	.41
Ther. exp. coeff.	10 <sup>-6</sup> in/in/°P(d)					
1		5.8	40.0	3.3	2.1	-2.5
2		5.8	40.0	10.7	20.1	39.6
Fracture stress	ksi(e)					
S <sub>TT</sub>		120(1) (1600)(2)	6(2)	220	187	200
S <sub>TC</sub>		120 (160)	10(3)	250	119	26
S <sub>LT</sub>		120 (160)	6	20	6.6	1.0
S <sub>2C</sub>		120 (160)	10	25	25.0	9.2
S <sub>3</sub>		70	7(3)	23	6.5	3.5

(1) 0.25 Offset yield strength; (2) Ultimate strength; (3) Estimated value.  
 Subscripts: 1 - Along fiber; 2 - Transverse to the fiber; 3 - Through-the-thickness;  
 T - Tension; C - Compression; S - Shear  
 Conversion factors: (a) Density: lb/in<sup>3</sup> x 27.68 = Gm/cm<sup>3</sup>; (b) Thickness: in. x 2.54 = cm;  
 (c) Modulus: 10<sup>6</sup> psi = 6.8948 GPa; (d) Ther. exp. coeff.:  
 10<sup>-6</sup> in/in/°P x 1.8 = 10<sup>-6</sup> cm/cm/°C; (e) Fracture stress:  
 ksi x 0.004848 x 10<sup>-2</sup> = GPa.

TABLE 3. - SUMMARY OF LAMINATION RESIDUAL PLY STRESSES (ksi)

[T = Δ - 300° F.]

Superhybrid <sup>a</sup>	Type of stress	Titanium plies			Adhesive plies			B/Al plies			KEV/E plies			S-G/E plies		
		Ply stress, ksi		MOS <sup>b</sup>	Ply stress, ksi		MOS	Ply stress, ksi		MOS	Ply stress, ksi		MOS	Ply stress, ksi		MOS
		Longi- tudinal	Trans- verse		Longi- tudinal	Trans- verse		Longi- tudinal	Trans- verse		Longi- tudinal	Trans- verse		Longi- tudinal	Trans- verse	
S-G (TYP)	Residual	3.88	-26.8	0.94	3.52	3.05	0.69	-2.46	-6.13	0.94	-----	-----	-----	-1.36	8.93	-0.84
KEV (TYP)	Residual	14.0	-23.4	0.93	3.66	3.10	0.67	16.6	-2.48	0.98	-10.7	5.08	-27.2	-----	-----	-----
S-G (3MOP)	Residual	4.10	-27.1	0.94	3.53	3.04	0.69	-1.92	-6.57	0.93	-----	-----	-----	-1.21	8.86	-0.81
KEV (3MOP)	Residual	14.3	-23.7	0.92	3.67	3.10	0.67	17.3	-2.88	0.97	-10.5	5.06	-27.0	-----	-----	-----
S-G (DT)	Residual	4.23	-27.1	0.94	3.53	3.04	0.69	-1.68	-6.59	0.93	-----	-----	-----	-1.14	8.85	-0.81
KEV (DT)	Residual	14.4	-23.6	0.92	3.67	3.10	0.67	17.6	-2.87	0.97	-10.4	5.07	-27.0	-----	-----	-----
S-G (DCT)	Residual	3.56	-34.6	0.91	3.51	2.94	0.70	-0.865	-16.1	0.59	-----	-----	-----	0.659	7.24	-0.21

<sup>a</sup>See table 1 for detailed description.

<sup>b</sup>MOS - margin of safety.



TABLE 5. - SUMMARY OF PLY INFLUENCE COEFFICIENTS DUE TO IN-PLANE TENSILE LOAD

Superhybrid <sup>a</sup>	Ply stress influence coefficients											
	Titanium plies		Boron/aluminum plies		S-glass/epoxy plies		KEV/EP plies		Adhesive plies			
	Longitudinal	Transverse	Longitudinal	Transverse	Longitudinal	Transverse	Longitudinal	Transverse	Longitudinal	Transverse		
S-G (TYP)	1.271	2.035	2.514	2.481	0.669	0.420	-----	-----	0.017	0.001		
KEV (TYP)	1.225	2.756	2.422	3.355	-----	-----	0.739	0.099	0.016	0.037		
S-G (3MOP)	1.472	1.875	2.907	2.175	0.775	0.368	-----	-----	0.020	0.024		
KEV (3MOP)	1.252	2.580	2.471	3.136	-----	-----	0.754	0.092	0.017	0.034		
S-G (DT)	1.297	2.058	2.555	2.504	0.690	0.421	-----	-----	0.017	0.028		
KEV (DT)	1.248	2.598	2.457	3.156	-----	-----	0.750	0.093	0.017	0.035		
S-G (DCT)	1.030	1.918	2.024	2.406	0.539	0.406	-----	-----	0.014	0.025		

<sup>a</sup>See table 1 for detailed description.

TABLE 6. - SUMMARY OF CONSTITUENTS PROPERTIES USED IN THE STRENGTH CALCULATIONS

Superhybrid <sup>a</sup>	Nongraphitic superhybrid			Titanium			Boron/aluminum				
	Total laminate, in.	Predicted laminate Modulus (ESH), 10 <sup>6</sup> psi		Thickness, in.	Modulus, 10 <sup>6</sup> psi	Strength		Longitude		Transverse	
		Longitudinal	Transverse			Yield, ksi	Ultimate, ksi	Modulus, 10 <sup>6</sup> psi	Strength, ksi	Modulus, 10 <sup>6</sup> psi	Strength, ksi
S-G (TYP)	0.068	13.4	8.34	0.0085	16	120	160	33	220	21	20
KEV (TYP)	0.075	13.6	6.46	0.0085	16	120	160	33	220	21	20
S-G (3MOP)	0.064	14.1	8.70	0.0077	16	120	160	33	220	21	20
KEV (3MOP)	0.071	14.2	6.64	0.0077	16	120	160	33	220	21	20
S-G (DT)	0.123	14.4	8.90	0.0137	16	120	160	33	220	21	20
KEV (DT)	0.137	14.5	6.76	0.0137	16	120	160	33	220	21	20
S-G (DCT)	0.110	12.9	7.29	0.0085	16	120	160	33	220	21	20

<sup>a</sup>See table 1 for detailed description.

Notes: TYP - typical for graphitic

3MOP - 3 mil thickness outer titanium ply

DT - double thickness

DCT - double core thickness

TABLE 7. - IN-PLANE STRENGTH COMPARISONS (ksi)

Superhybrid <sup>a</sup>	Longitudinal strength			Transverse strength		
	Predicted		Experi- mental	Predicted		Experi- mental
	Upper bound	Lower bound		Upper bound	Lower bound	
S-G (TYP)	126	96.0	107	26.1	20.0	25.0
KEV (TYP)	131	96.7	102	22.6	16.1	27.9
S-G (3MOP)	109	103	108	32.7	26.9	30.2
KEV (3MOP)	128	103	119	29.0	25.0	25.7
S-G (DT)	123	103	128	27.6	21.1	24.0
KEV (DT)	128	103	105	24.4	19.9	24.4
S-G (DCT)	155	91.0	165	20.5	14.9	17.0

<sup>a</sup>See table 1 for detailed description.

**TABLE 8. - SUMMARY OF COMPARISONS FOR TRANSVERSE  
STRESS-STRAIN BEHAVIOR**

Superhybrid <sup>a</sup>	Composite stress, ksi at:						
	First knee		Second knee		Fracture		
	Pre-dicted <sup>(1)</sup>	Experi-mental <sup>(2)</sup>	Pre-dicted <sup>(3)</sup>	Experi-mental <sup>(4)</sup>	Predicted <sup>(5)</sup>		Experi-mental <sup>(6)</sup>
					Upper bound	Lower bound	
S-G (TYP)	8.1	9	21.2	21	26.1	20.0	28.3
KEV (TYP)	6.0	3	19.9	22	22.6	18.1	27.9
S-G (3MOP)	9.2	7	26.8	26	32.7	26.9	30.2
KEV (3MOP)	6.4	3	22.7	21	29.0	25.0	25.7
S-G (DT)	8.0	9	21.8	18	27.6	21.1	24.0
KEV (DT)	6.3	4	19.3	18	24.4	19.9	24.4
S-G (DCT)	8.3	6	18.0	14	20.5	14.9	17.0

<sup>a</sup>See table 1 for detailed description.

Notes: (1) Predicted - B/Al ply failure

(2) Estimated stress from transverse stress-strain curves - initial portion (figs. 1 to 7)

(3) Predicted - titanium ply yield

(4) Estimated - stress from transverse stress-strain curves - final portion (figs. 1 to 7)

(5) From table 7

(6) From stress-strain curves

TABLE 9. - SUMMARY OF CALCULATED OUTER PLY STRESSES (ksi) DUE TO 3-POINT BENDING FRACTURE LOAD  
(OUTER PLYS ON TENSION SIDE)

Superhybrid <sup>a</sup>	Flexural strength		Titanium ply			Adhesive ply			B/AI ply			S-G/E ply			KEV 49/E ply		
	Direction	ksi	Longitudinal	Transverse	MOS	Longitudinal	Transverse	MOS	Longitudinal	Transverse	MOS	Longitudinal	Transverse	MOS	Longitudinal	Transverse	MOS
S-G (TYP)	Longitudinal	167	170.	5.62	-0.95	2.16	0.30	0.89	239.	-2.95	-0.30	42.1	-0.68	0.94	---	---	---
	Transverse	81	12.6	115	.17	.31	1.44	.95	-5.41	103.	-25.6	-2.85	11.5	-2.06	---	---	---
KEV (TYP)	Longitudinal	168	170.	5.14	-0.95	2.16	0.30	0.88	248.	-3.51	-0.43	---	---	---	51.8	0.47	0.84
	Transverse	81	15.3	124	.04	.36	1.56	.94	-3.57	116	-32.5	---	---	---	-5.79	2.31	-4.92
S-G (3MOP)	Longitudinal	175	162.	5.78	-0.76	2.00	0.28	0.90	247.	-2.63	-0.38	43.6	-0.66	0.94	---	---	---
	Transverse	64	9.71	84.4	.56	.23	1.03	.98	-3.58	82.3	-16.0	-2.14	9.19	.96	---	---	---
KEV (3MOP)	Longitudinal	192	168.	5.47	-0.89	2.09	0.29	0.89	264.	-3.34	-0.60	---	---	---	55.2	0.51	0.82
	Transverse	64	11.2	87.2	.53	.25	1.07	.97	-1.92	87.7	-18.2	---	---	---	-4.22	1.75	-2.40
S-G (DT)	Longitudinal	162	159.	5.60	-0.69	2.04	0.29	0.90	254.	-2.77	-0.45	44.0	-0.67	0.94	---	---	---
	Transverse	66	10.5	91.8	.47	.26	1.16	.97	-4.22	93.6	-21.0	-2.43	10.3	-1.46	---	---	---
KEV (DT)	Longitudinal	172	154.	4.98	-0.59	1.98	0.28	0.90	252.	-3.21	-0.45	---	---	---	52.7	0.49	0.83
	Transverse	65	11.5	89.7	.50	.27	1.14	.97	-2.22	93.7	-21.0	---	---	---	-4.56	1.88	-2.90
S-G (DCT)	Longitudinal	153	120	4.88	0.04	1.56	0.23	0.94	196.	-1.47	0.16	42.8	-0.56	0.94	---	---	---
	Transverse	59	9.41	71.3	.69	.22	.91	.98	-1.25	74.2	-12.8	-1.97	10.3	-1.44	---	---	---

<sup>a</sup>See table 1 for detailed description.

TABLE 10. - SUMMARY OF INFLUENCE COEFFICIENTS DUE TO FLEXURAL LOAD

Superhybrid <sup>a</sup>	Ply stress influence coefficients <sup>(1)</sup>											
	Titanium		Adhesive		Boron/aluminum		S-G/EP		KEV/EP			
	Longi- tudinal <sup>(2)</sup>	Trans- verse <sup>(3)</sup>	Longi- tudinal	Trans- verse	Longi- tudinal	Trans- verse	Longi- tudinal	Trans- verse	Longi- tudinal	Trans- verse		
S-G (TYP)	1.018 (4) (0.98)	1.420 (1.35)	0.013	0.018	1.431	1.272	0.252	0.142	-----	-----	-----	
KEV (TYP)	1.012 (0.87)	1.531 (1.46)	0.013	0.019	1.476 (1.33)	1.432	-----	-----	0.308	0.026	-----	
S-G (3MOP)	0.926	1.390	0.012	0.016	1.411	1.286	0.249	0.144	-----	-----	-----	
KEV (3MOP)	0.875	1.362	0.010	0.017	1.375	1.370	-----	-----	0.288	0.027	-----	
S-G (DT)	0.981 (0.96)	1.391 (1.35)	0.013	0.018	1.568 (1.42)	1.418 (1.24)	0.272	0.156	-----	-----	-----	
KEV (DT)	0.895 (0.86)	1.380 (1.32)	0.012	0.018	1.465 (1.34)	1.442 (1.32)	-----	-----	0.306	0.029	-----	
S-G (DCT)	0.784 (0.76)	1.208 (1.17)	0.010	0.015	1.281	1.258	0.280	0.175	-----	-----	-----	

<sup>a</sup>See table 1 for detailed description.

Notes: (1) Firstly-encountered ply from the surface inward

(2) Composite and ply stress along fiber direction

(3) Composite and ply stress transverse to fiber direction

(4) Value in parenthesis is average of two outer plies and was used in the strength predictions

**TABLE 11. - SUMMARY OF COMPARISONS FOR FLEXURAL STRENGTH**

Superhybrid <sup>a</sup>	Flexural strength, ksi					
	Longitudinal			Transverse		
	Predicted		Experi- mental <sup>(3)</sup>	Predicted		Experi- mental <sup>(3)</sup>
	Upper bound <sup>(1)</sup>	Lower bound <sup>(2)</sup>		Upper bound <sup>(4)</sup>	Lower bound <sup>(5)</sup>	
S-G (TYP)	163	154	167	89	54	81
KEV (TYP)	184	165	186	82	49	81
S-G (3MOP)	172	156	175	92	52	64
KEV (3MOP)	182	159	192	88	49	61
S-G (DT)	167	155	162	89	53	66
KEV (DT)	186	164	172	91	50	65
S-G (DCT)	210	172	153	103	42	59

<sup>a</sup>See table 1 for detailed description.

- Notes: (1) Titanium plies fracture  
 (2) B/Al plies fracture  
 (3) From reference 1, table 4  
 (4) Titanium plies fracture  
 (5) B/Al and titanium plies fracture

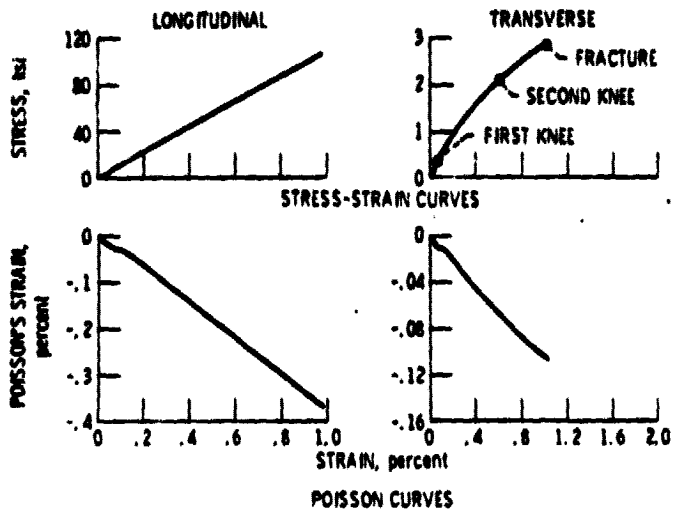


Figure 1. - Stress-strain and Poisson's strain curves for NGSB S-G (TYP) composite. (Refer to table 1 for laminate configuration.)

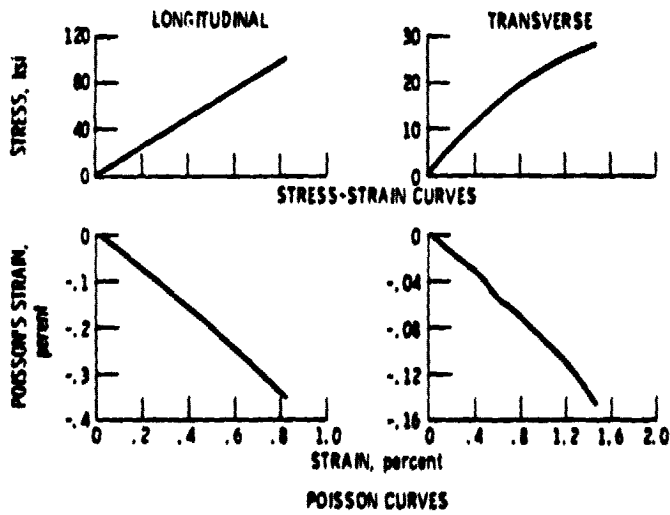


Figure 2. - Stress-strain and Poisson's strain curves for NGSB KEV (TYP) composite. (Refer to table 1 for laminate configuration.)

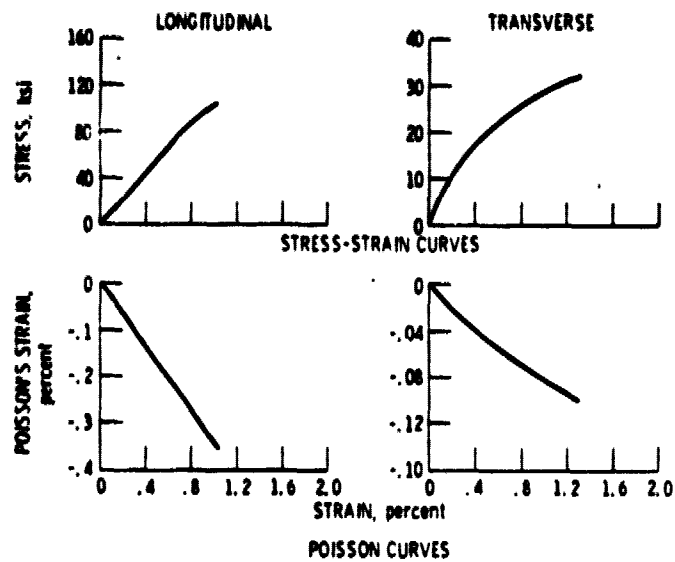


Figure 3. - Stress-strain and Poisson's strain curves for NGSB S-G (3MOP) composite. (Refer to table 1 for laminate configuration.)

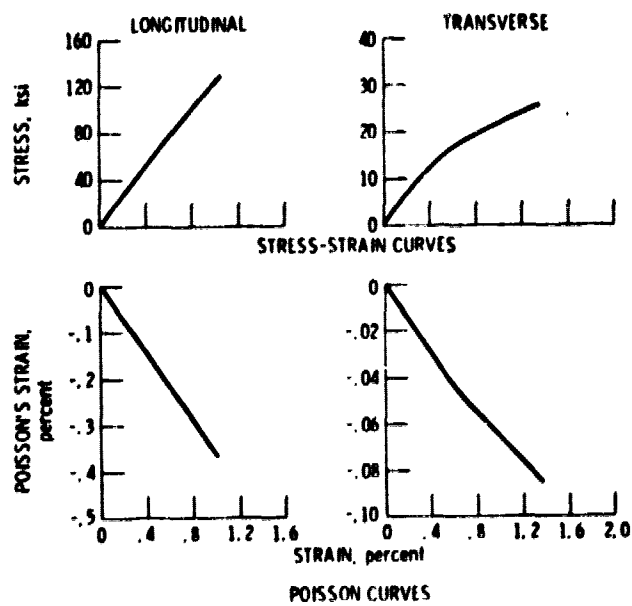


Figure 4. - Stress-strain and Poisson's strain curves for NGSB K1V (3MOP) composite. (Refer to table 1 for laminate configuration.)

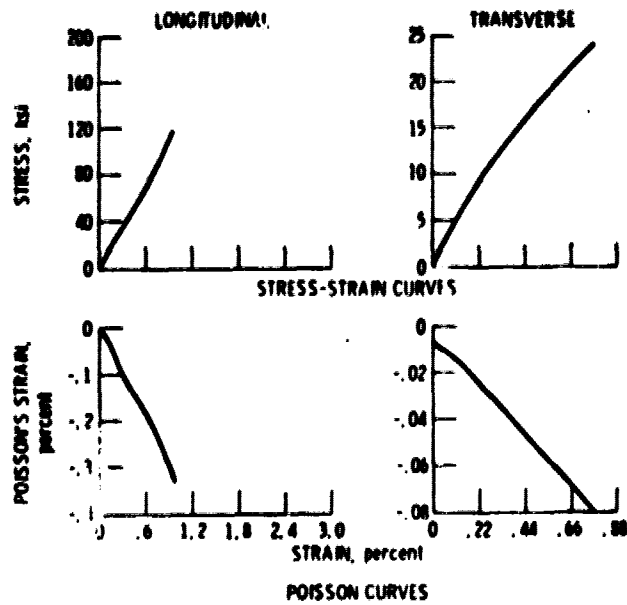


Figure 5. - Stress-strain and Poisson's strain curves for NGSB S-G (DT) composite. (Refer to table 1 for laminate configuration.)

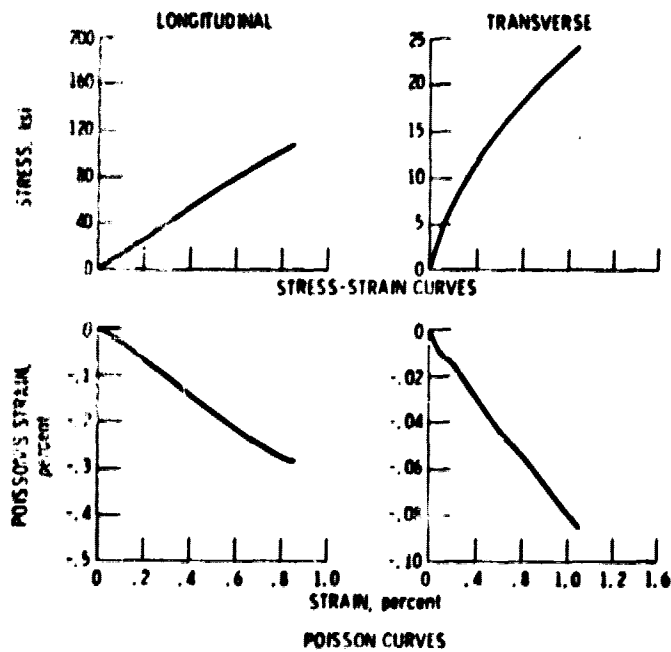


Figure 6. - Stress-strain and Poisson's strain curves for NGSB KEV (DT) composite. (Refer to table 1 for laminate configuration.)

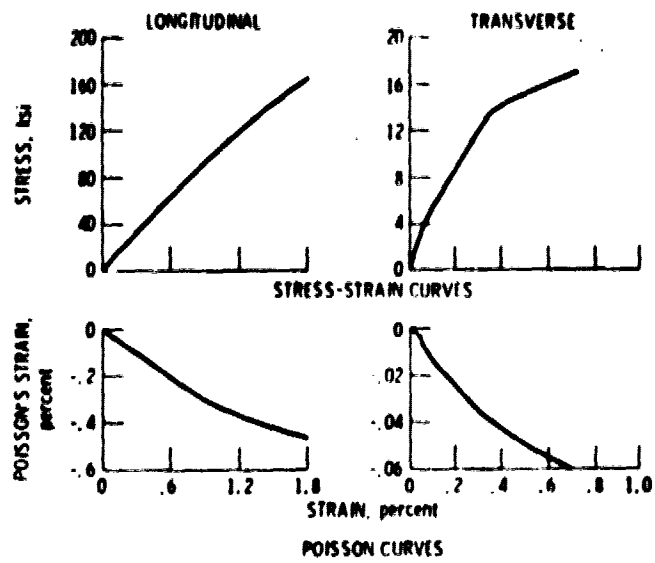


Figure 7. - Stress-strain and Poisson's strain curves for NCSH  
S G (DCT) composite. (Refer to table for laminate configura-  
tion.)